

Electrosynthesis of Ammonia with High Selectivity and High Rates via Engineering of the Solid-Electrolyte Interphase. *Joule* 6, 2083–2101.

8. Du, H.-L., Chatti, M., Hodgetts, R.Y., Cherepanov, P.V., Nguyen, C.K., Matuszek, K., MacFarlane, D.R., and Simonov, A.N. (2022). Electroreduction of nitrogen at almost 100% current-to-ammonia efficiency.

*Nature*. <https://doi.org/10.1038/s41586-022-05108-y>.

9. Li, K., Shapel, S.G., Hochfilzer, D., Pedersen, J.B., Krempel, K., Andersen, S.Z., Sažinas, R., Saccoccio, M., Li, S., Chakraborty, D., et al. (2022). Increasing Current Density of Li-Mediated Ammonia Synthesis with High Surface Area Copper Electrodes. *ACS Energy Lett.* 7, 36–41.

<https://doi.org/10.1021/acscenergylett.1c02104>.

10. Lazouski, N., Chung, M., Williams, K., Gala, M.L., and Manthiram, K. (2020). Non-aqueous gas diffusion electrodes for rapid ammonia synthesis from nitrogen and water-splitting-derived hydrogen. *Nat. Catal.* 3, 463–469. <https://doi.org/10.1038/s41929-020-0455-8>.

## Solid-electrolyte interphases enable efficient Li-mediated ammonia electrosynthesis

Yifu Chen,<sup>1</sup> Shuang Gu,<sup>2</sup> and Wenzhen Li<sup>1,\*</sup>

**The function and composition of solid-electrolyte interphases in lithium-mediated ammonia electrosynthesis are important yet largely unknown. Recently in *Joule* and *Nature*, Chorkendorff, Simonov, and their colleagues demonstrated that engineering the solid-electrolyte interphases is essential to boosting ammonia electrosynthesis up to a record-high rate and current efficiency.**

As a landmark achievement in the modern chemical industry, the Haber-Bosch (H-B) process nowadays fixes around 150 million metric tons of atmospheric dinitrogen (N<sub>2</sub>) annually into ammonia (NH<sub>3</sub>),<sup>1</sup> accounting for 40% of the total N-nutrient circulated in the global nitrogen cycle.<sup>2</sup> Despite being highly energy-efficient, the traditional H-B process is becoming less and less suitable within the context of sustainability because the required hydrogen (H<sub>2</sub>) reactant is derived from fossil fuels: either methane (via steam methane reforming) or coal. Operated under extremely harsh conditions (450°C–550°C and 250–350 bar) in centralized plants, the H-B process lacks the flexibility in economical deployment in smaller-scale facilities for the “distributed” NH<sub>3</sub> production—a long pursuit that aims to significantly bring down its transportation cost, especially for the less-developed regions of the world.

On that account, the electrochemical nitrogen reduction reaction (NRR) has been suggested as a promising alternative NH<sub>3</sub>-producing process, since it does not rely on fossil-derived H<sub>2</sub>. The past few years have witnessed a reckless “gold rush” on claiming a glut of electrocatalytic materials putatively active for aqueous NRR, but their performances are far from satisfactory due to sluggish NRR kinetics and the low N<sub>2</sub> solubility in aqueous electrolytes; more concerning is the validation of those subtle NRR activities as questioned by several individual reports.<sup>3,4</sup>

So far, this debate has led to a common recognition that currently only an indirect lithium (Li)-mediated approach (Figure 1) consistently manifests its validity in electrochemically reducing N<sub>2</sub> under varying conditions. In fact, Li is the only metal that is capable of cleaving the N≡N bond under ambient conditions. This Li-mediated approach

dates back to 1993 in the groundbreaking work by Sakata and colleagues.<sup>5</sup> As shown in Figure 1A, the three basic steps of Li-NRR can be brought together in the solid-electrolyte interphase (SEI) region of a single electrolytic cell in the presence of a Li<sup>+</sup>-containing electrolyte, N<sub>2</sub> reactant, and a soluble proton carrier (HA). In traditional Li-ion batteries, SEI is a layer of material that forms between the negative electrode and the liquid electrolyte, and it is generated spontaneously by the breakdown of electrolyte compounds during the first few charging cycles under highly reducing potentials. SEI in those batteries provides the passivation of the negative electrode, inhibiting further electrolyte decomposition as well as suppressing the formation of lithium dendrites. A similar SEI may exist in Li-NRR system, but its composition and function are largely unknown.

In this issue of *Joule*, Chorkendorff and colleagues<sup>6</sup> reported an unprecedented NH<sub>3</sub> production rate of 2,500 nmol cm<sup>-2</sup> s<sup>-1</sup> with a current-to-NH<sub>3</sub> efficiency of 71% achieved with a stable SEI layer created by LiBF<sub>4</sub> electrolyte. Within the same month in *Nature*, Simonov and colleagues<sup>7</sup>

<sup>1</sup>Department of Chemical and Biological Engineering, Iowa State University, Ames, IA 50011, USA

<sup>2</sup>Department of Mechanical Engineering, Wichita State University, Wichita, KS 67260, USA

\*Correspondence: [wzli@iastate.edu](mailto:wzli@iastate.edu)  
<https://doi.org/10.1016/j.joule.2022.08.013>



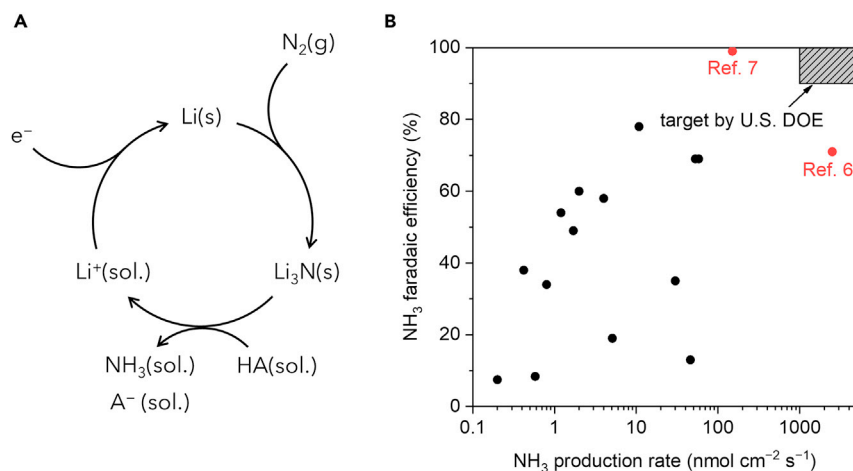


**Figure 1. An overview of Li-NRR**

(A) The reactions involved in the Li-NRR process, including the electro-reduction of  $\text{Li}^+$  to  $\text{Li}(0)$ , the nitridation of  $\text{Li}(0)$  to  $\text{Li}_3\text{N}$ , and the protonation of  $\text{Li}_3\text{N}$  to  $\text{NH}_3$  and  $\text{Li}^+$ . (s), (g), and (sol.) represent the solid, gas, and solution phase, respectively. Adapted with permission from Lazouski et al.<sup>10</sup> (B) The Li-NRR performances in previous reports (black) and the two highlighted works (red). Data are obtained from Du et al.<sup>7</sup> The gray patterned zone represents the targets projected by the US Department of Energy.<sup>8</sup>

published their findings of the close-to-unity (99%) faradaic efficiency (FE) toward  $\text{NH}_3$  spanning 4 days enabled by a compact SEI layer created by concentrated bis(trifluoromethylsulfonyl)imide ( $\text{NTf}_2^-$ ) electrolyte, albeit at a lower production rate of  $150 \text{ nmol cm}^{-2} \text{ s}^{-1}$ . The performances from the two systems are approaching the US Department of Energy target for  $\text{NH}_3$  electro-synthesis:  $>1,000 \text{ nmol cm}^{-2} \text{ s}^{-1}$  of  $\text{NH}_3$  production rate with  $>90\%$  of FE (Figure 1B).<sup>8</sup>

As illustrated in Figure 2A, Chorkendorff and colleagues in this *Joule* article elaborated the distinct function of SEI in the Li-NRR systems: determining the relative diffusion rates ( $r$ ) of  $\text{Li}^+$ ,  $\text{H}^+$ , and  $\text{N}_2$  in addition to the traditional function as electrode passivation for electrolyte protection and dendrite suppression (similar in Li-ion batteries). Raising the ratio of diffusion rate of  $\text{N}_2$  to  $\text{Li}^+$  ( $r_{\text{N}_2}/r_{\text{Li}^+}$ ) and/or the ratio of diffusion rate of  $\text{H}^+$  to  $\text{Li}^+$  ( $r_{\text{H}^+}/r_{\text{Li}^+}$ ) effectively increases FE. Upon screening a series of Li-compounds, the authors discovered that fluorides ( $\text{LiHF}_2$  and  $\text{LiF}$ ) are the most stable insoluble phases in the SEI

layer when  $\text{LiBF}_4$  is used as the electrolyte. First-principles study on the possible defect formation suggested that the  $\text{Li}^+$  conductivity in fluorides is several orders of magnitude lower than that in  $\text{Li}_2\text{CO}_3$ , thereby raising both ( $r_{\text{N}_2}/r_{\text{Li}^+}$ ) and ( $r_{\text{H}^+}/r_{\text{Li}^+}$ ) for high FE at large current density (both  $r_{\text{N}_2}$  and  $r_{\text{H}^+}$  do not experience large changes). In addition, the migration of surface  $\text{Li}^+$  exhibits a lower barrier (0.09 eV) compared to  $\text{LiOH}$  (0.22 eV) and  $\text{Li}_2\text{CO}_3$  (0.3 eV), which promotes the in-plane migration of  $\text{Li}^+$  on the surface rendering a stable and smooth LiF-enriched SEI layer, responsible for stable Li-NRR operation.

A porous Cu electrode with a 308-fold electrochemically active surface area versus its geometric area was prepared to allow for stable cell operation at ultrahigh current densities such as  $1.0 \text{ A cm}^{-2}$ . Thanks to the stable SEI created by  $\text{LiBF}_4$  electrolyte, high FE of 71% was demonstrated at this unprecedented current density, delivering the record-high  $\text{NH}_3$  production rate of  $2,500 \text{ nmol cm}^{-2} \text{ s}^{-1}$ . Under the same test conditions, the SEI created by

$\text{LiPF}_6$  or  $\text{LiClO}_4$  is apparently less stable (Figure 2B).

To unveil the chemical composition of the SEI layer created by different electrolytes, a procedure was established to preserve the SEI structure without air exposure or peel-off upon depressurizing for X-ray photoelectron spectroscopy (XPS) and X-ray diffraction (XRD) studies. The characterization results confirmed the LiF-enriched nature of the SEI with  $\text{LiBF}_4$  and  $\text{LiPF}_6$  throughout the period of electrolysis in concert with the theoretically suggested optimal case.

In the *Nature* article, Simonov and colleagues introduced a new class of electrolyte based on imide “lithium bis(trifluoromethylsulfonyl)imide,” or  $\text{LiNTf}_2$  in Li-NRR system, to create a compact SEI layer for ultrahigh FE. As shown in Figure 2C, higher  $\text{LiNTf}_2$  concentration leads to higher FE toward  $\text{NH}_3$ , presumably through thickening the SEI layer. Meanwhile, the  $\text{NH}_3$  production rate peaks between 1.5 and 2.0 M  $\text{LiNTf}_2$ , likely because of the interplay among rising FE, rising SEI resistance, changing electrolyte conductivity (first increase and then decrease), and the resultant current density under the fixed cathode potential of  $-0.55 \text{ V}$  versus  $\text{Li}/\text{Li}^+$ . Specifically using 2.0 M  $\text{LiNTf}_2$  to create a compact yet efficient SEI layer, almost 100% of FE with  $150 \text{ nmol cm}^{-2} \text{ s}^{-1}$  of  $\text{NH}_3$  production rate was demonstrated on a Ni electrode in stable operation for 96 h. In their cell system under the same test conditions (2 M),  $\text{LiNTf}_2$  brought higher FE than the smaller imide-based analog LiFSI (lithium bis(fluorosulfonyl)imide) and other common electrolytes such as  $\text{LiBF}_4$ ,  $\text{LiClO}_4$ , and LiOTf (lithium triflate).

Unlike the SEI created by  $\text{LiBF}_4$  or  $\text{LiPF}_6$  through the spontaneous decomposition of electrolytes, the  $\text{LiNTf}_2$ -induced SEI layer may be constituted of high-concentration of electrolyte itself

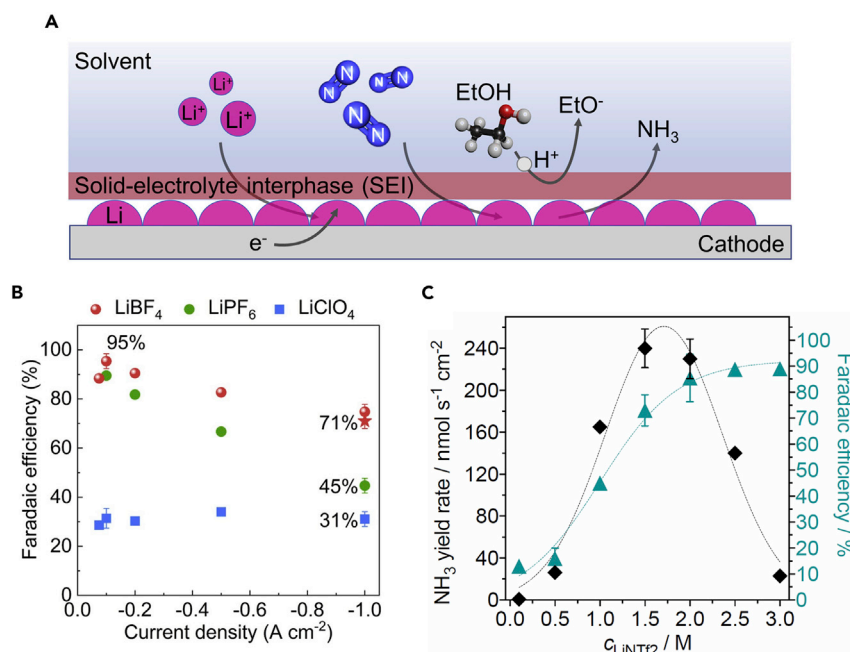


**Figure 2. Engineering the SEI layer for high-performance Li-NRR**

(A) Schematic illustration of Li-NRR at the SEI region of the electrode. An ideal SEI layer for Li-NRR allows for the efficient transport of Li<sup>+</sup>, N<sub>2</sub>, and NH<sub>3</sub> while preventing the direct contact of the proton carrier (ethanol) with the Li deposit, which causes the Li-consuming side reaction. Reprinted with permission from Li et al.<sup>6</sup>

(B) FE toward NH<sub>3</sub> with different lithium salts reported by Chorkendorff and colleagues.<sup>6</sup>

(C) Li-NRR performance with different concentrations of LiNTf<sub>2</sub> reported by Simonov and colleagues.<sup>7</sup>

with layers of strongly coordinated Li<sup>+</sup> and NTf<sub>2</sub><sup>-</sup> ions through a tight and chelate-type binding. This is supported by an order of magnitude higher interfacial capacitance as measured in the Li-NRR system. Further, the interfacial capacitance follows the LiNTf<sub>2</sub> concentration (in the range of 0.5–2.0 M). The SEI layer created by LiNTf<sub>2</sub> was found to be stable under cathode potential as negative as –0.8 V versus Li/Li<sup>+</sup>.

Successful demonstration of the unprecedentedly high-performance Li-NRR in the two works has unquestionably brought us one step closer to transforming the H-B process into a more sustainable and flexible electrochemical alternative for NH<sub>3</sub> synthesis.

Notwithstanding the efficient SEI engineering at the cathode for enhanced Li-NRR, the major problem of all Li-NRR sys-

tems thus far arises from the anode, where the solvent (tetrahydrofuran) serves as a sacrificial agent to offer electron and proton to complete the overall reaction. Oxidation of H<sub>2</sub> appears to be a viable option, and it has been demonstrated to prevent the oxidation of tetrahydrofuran,<sup>9</sup> but the use of H<sub>2</sub> brings about new problems regarding the additional cost and sustainability of H<sub>2</sub> production, along with the transportation and handling of H<sub>2</sub>. The continuously consumed anodic reactant is required to be both sustainable and compatible with NH<sub>3</sub> production.

While achieving those record-high performances, very high cell voltage was observed in both systems (10 and 7 V), largely from high anode overpotential. In addition, high N<sub>2</sub> pressure (20 or 15 bar) was employed to secure high performance in both works.

The readers should note that the generated NH<sub>3</sub> from Li-NRR systems in both works are largely dissolved in their electrolytes. Thus, subsequent separation of the NH<sub>3</sub> product of Li-NRR is an important next-step challenge for which Chorkendorff and colleagues suggested transitioning the Li-NRR process from the batch-type reactor into a flow reactor with continuous N<sub>2</sub> feed. Nonetheless, the high pressure of N<sub>2</sub> may also challenge this transition.

Techno-economic analysis (TEA) is critically needed to carefully examine the possibility of the Li-NRR approach for practical real-world applications through identifying the barriers and requirements in terms of energy consumption, materials costs (electrodes, electrolyte, and reactants), product separation, and pressure management. The TEA study should guide future research in promising directions.

## DECLARATION OF INTERESTS

The authors declare no competing interests.

## REFERENCES

1. Apodaca, L. (2022). Nitrogen (Fixed)—Ammonia (U.S. Geological Survey).
2. Fowler, D., Coyle, M., Skiba, U., Sutton, M.A., Cape, J.N., Reis, S., Sheppard, L.J., Jenkins, A., Grizzetti, B., Galloway, J.N., et al. (2013). The global nitrogen cycle in the twenty-first century. *Phil. Trans. R. Soc. B* 368, 20130164. <https://doi.org/10.1098/rstb.2013.0164>.
3. Andersen, S.Z., Čolić, V., Yang, S., Schwalbe, J.A., Nielander, A.C., McEnaney, J.M., Enemark-Rasmussen, K., Baker, J.G., Singh, A.R., Rohr, B.A., et al. (2019). A rigorous electrochemical ammonia synthesis protocol with quantitative isotope measurements. *Nature* 570, 504–508. <https://doi.org/10.1038/s41586-019-1260-x>.
4. Choi, J., Suryanto, B.H.R., Wang, D., Du, H.-L., Hodgetts, R.Y., Ferrero Vallana, F.M., MacFarlane, D.R., and Simonov, A.N. (2020). Identification and elimination of false positives in electrochemical nitrogen reduction studies. *Nat. Commun.* 11, 5546. <https://doi.org/10.1038/s41467-020-19130-z>.
5. Tsuneto, A., Kudo, A., and Sakata, T. (1993). Efficient Electrochemical Reduction of N<sub>2</sub> to NH<sub>3</sub> Catalyzed by Lithium. *Chem. Lett.* 22, 851–854. <https://doi.org/10.1246/cl.1993.851>.
6. Li, S., Zhou, Y., Li, K., Saccoccio, M., Sažinas, R., Andersen, S.Z., Pedersen, J.B., Fu, X.,

- Shadravan, V., Chakraborty, D., et al. (2022). Electrosynthesis of ammonia with high selectivity and high rates via engineering of the solid-electrolyte interphase. *Joule* 6, 2083–2101. <https://doi.org/10.1016/j.joule.2022.07.009>.
7. Du, H.-L., Chatti, M., Hodgetts, R.Y., Cherepanov, P. v, Nguyen, C.K., Matuszek, K., MacFarlane, D.R., and Simonov, A.N. (2022). Electroreduction of nitrogen at almost 100% current-to-ammonia efficiency. *Nature*. <https://doi.org/10.1038/s41586-022-05108-y>.
8. Advanced Research Projects Agency–Energy. (2016). Renewable Energy to Fuels through Utilization of Energy-Dense Liquids (REFUEL). [https://arpa-e.energy.gov/sites/default/files/documents/files/REFUEL\\_ProgramOverview.pdf](https://arpa-e.energy.gov/sites/default/files/documents/files/REFUEL_ProgramOverview.pdf).
9. Lazouski, N., Chung, M., Williams, K., Gala, M.L., and Manthiram, K. (2020). Non-aqueous gas diffusion electrodes for rapid ammonia synthesis from nitrogen and water-splitting-derived hydrogen. *Nat. Catal.* 3, 463–469. <https://doi.org/10.1038/s41929-020-0455-8>.
10. Lazouski, N., Schiffer, Z.J., Williams, K., and Manthiram, K. (2019). Understanding Continuous Lithium-Mediated Electrochemical Nitrogen Reduction. *Joule* 3, 1127–1139. <https://doi.org/10.1016/j.joule.2019.02.003>.

## How to find an ideal thermoelectric material

Dan Zhao<sup>1,\*</sup>

**Ionic thermoelectric materials have recently aroused intense research interest because of their promising potential for heat energy conversion. In a recent *Cell Reports Physical Science* article, Ma et al. presented a comprehensive study of the evaluation parameters from the view of field evolutions of temperature, voltage, and ionic concentration.**

Using the thermoelectric effect to convert heat into electricity is the dream approach to recovering waste heat from heat engines and industry dissipation, harvesting clean solar energy, and powering mobile/remote devices without maintenance. The main challenge in the development of a viable thermoelectric technology is the high material and manufacturing costs compared to the relatively low efficiency. For classic thermoelectric materials based on semi-conducting metal alloys, it is difficult to further reduce these costs because they are composed of scarce, nonrenewable elements that require restrictive processing methods.

In this context, solution-processable electrolytes that are composed of earth-abundant elements are assuredly the ideal substitution materials. In addition to advantages of low-cost and environmentally friendly compositions,

some electrolytes possess large Seebeck coefficients (the ratio between thermal voltage and applied temperature difference) typically in the range of 5 mV/K–30 mV/K,<sup>1</sup> and these electrolytes are addressed as ionic thermoelectric materials. Their ability to generate large voltages is especially beneficial for charging supercapacitors or batteries since the stored energy density increases quadratically with the charging voltage.<sup>2</sup> In turn, the possibility of converting heat into electricity by charging a supercapacitor has promoted the exploration of electrolytes with large Seebeck coefficients and diverse mechanical properties that enable wide ranged application.<sup>3–5</sup> The figure of merit  $ZT_i = \alpha_i \sigma_i / \kappa$  of ionic thermoelectric materials was derived using the generated thermal voltage to charge a supercapacitor, which is connected to the efficiency of the ionic thermoelectric supercapacitor (ITESC) based on such electrolytes.<sup>6</sup>

$$\eta_{\text{ch}} = \frac{\Delta T}{T_{\text{H}}} \frac{ZT_i}{2ZT_i + \frac{10T}{T_{\text{H}}} - \frac{1}{2}ZT_i \frac{\Delta T}{T_{\text{H}}}}$$

Such  $ZT_i$  enables direct comparison of ionic thermoelectric materials with traditional electronic materials when using them to charge the same supercapacitor, and it defines basic parameters of a good ionic thermoelectric material. Nevertheless, the calculation of efficiency is based on simplified device operation in which only the input heat during the charging process, after the establishment of a temperature gradient and thermal voltage, was included. However, the neglected heat used to generate the temperature gradient and thermal voltage constitutes the majority of the input energy and is not easy to practically recycle. In other words, the speed of establishing a temperature gradient and the corresponding thermal voltage along the device is actually the key to determining the efficiency of ionic thermoelectric materials (as illustrated in Figure 1).

Writing in *Cell Reports Physical Science*, Ma et al.<sup>7</sup> accounted for this and built a practical expression of the figure of merit of ionic thermoelectric materials by analyzing the net charge accumulation and temperature field

<sup>1</sup>Laboratory of Organic Electronics, Department of Science and Technology, Linköping University, 601 74 Norrköping, Sweden

\*Correspondence: [dan.zhao@liu.se](mailto:dan.zhao@liu.se)  
<https://doi.org/10.1016/j.joule.2022.08.017>

